Pérez-Martínez, FC.; Carrión, B.; Lucío, MI.; Rubio, N.; Herrero, MA.; Vázquez, E.; Ceña, V. (2012). Enhanced docetaxel-mediated cytotoxicity in human prostate cancer cells through knockdown of cofilin-1 by carbon nanohorns delivered siRNA. Biomaterials. 33(32):8152-8159. https://doi.org/10.1016/j.biomaterials.2012.07.038

Enhanced docetaxel-mediated cytotoxicity in human prostate cancer cells through knockdown of cofilin-1 by carbon nanohorn delivered siRNA

Francisco C. Pérez-Martínez [a], Blanca Carrión [a], Maria I. Lucío [b], Noelia Rubio [b], María A. Herrero [b], Ester Vázquez [b], Valentín Ceña [c,d,*]

[a] NanoDrugs, S.L. Parque Científico y Tecnológico, 02071 Albacete, Spain
[b] Área de Química Orgánica, Facultad de Química-IRICA, Universidad de Castilla-La Mancha, 13071 Ciudad Real, Spain
[c] Unidad Asociada Neurodeath, CSIC-Universidad de Castilla-La Mancha, Facultad de Medicina, 02006 Albacete, Spain
[d] CIBERNED, Instituto de Salud Carlos III, 28029 Madrid, Spain

Keywords:
Dendrimer
Gene therapy nanoparticle
siRNA
Prostate cancer

A B S T R A C T

We synthesized a non-viral delivery system (*f*-CNH3) for small interfering RNA (siRNA) by anchoring a fourth-generation polyamidoamine dendrimer (G4-PAMAM) to carbon nanohorns (CNHs). Using this new compound, we delivered a specific siRNA designed to knockdown cofilin-1, a key protein in the regulation of cellular cytoskeleton, to human prostate cancer (PCa) cells. The carbon nanohorn (CNH) derivative was able to bind siRNA and release it in the presence of an excess of the polyanion heparin. Moreover, this hybrid nanomaterial protected the siRNA from RNAse-mediated degradation. Synthetic siRNA delivered to PCa cells by *f*-CNH3 decreased the cofilin-1 mRNA and protein levels to about 20% of control values. Docetaxel, the drug of choice for the treatment of PCa, produced a concentration-dependent activation of caspase-3, an increase in cell death assessed by lactate dehydrogenase release to the culture medium, cell cycle arrest and inhibition of tumor cell proliferation. All of these toxic effects were potentiated when cofilin-1 was down regulated in these cells by a siRNA delivered by the nanoparticle. This suggests that knocking down certain proteins involved in cancer cell survival and/or proliferation may potentiate the cytotoxic actions of anticancer drugs and it might be a new therapeutic approach to treat tumors.

1. Introduction

Prostate cancer (PCa) is one of the main causes of death among men in the Western world. Autopsy series have revealed that small prostatic carcinomas are present in up to 64 percent of men from 60 to 70 years of age [1]. Moreover, the risk of death due to metastatic PCa is 1 in 30 [2]. Current treatments attempt to block PCa cell growth and induce cell death [3], but the progression of advanced PCa to hormone independence is only temporally disrupted by therapeutic interventions including androgen ablation therapy or chemotherapy [4]. Docetaxel, an antimitotic cytotoxic drug belonging to the taxoid family, is used as the gold-standard therapy for patients with advanced PCa [5]. Docetaxel's anticancer effects are associated with its ability to induce the polymerization of tubulin, which impairs cell proliferation, which in turn leads to mitotic arrest and apoptosis [6,7]. However, docetaxel-based chemotherapy has undesirable side effects that limit the tolerated dose and may reduce the therapeutic efficacy [8]. This result suggests that coadjuvant therapy leading to a reduction of the required dose of docetaxel would be beneficial to PCa therapy. One possible approach is to knockdown proteins involved in cancer cell survival or proliferation using specific RNA interference (RNAi) [9].

Dynamic changes in the actin cytoskeleton, such as depolymerization and severing of actin filaments, are essential for several cellular processes including cell survival, shaping, cytokinesis, migration and chemotaxis [10] suggesting that the cytoskeleton is a potential target for cancer therapies [11,12]. The actin depolymerizing factor (ADF)/cofilin has emerged as one of the protein families that regulates actin and cytoskeleton dynamics [13]. Furthermore, cofilin type 1 (cofilin-1) is an ubiquitous protein regulating various cell functions, such as cell cycle control and proliferation [14], apoptosis [15] and excitotoxic neurodegeneration [16]. In addition, enhanced amounts of cofilin-1 are related to the progression of some types of tumors and metastases [17e19] suggesting that cofilin-1 knockdown may have therapeutic benefits when combined with antitumoral drugs in cancer therapy.

* Corresponding author. Unidad Asociada Neurodeath, Facultad de Medicina, Avda. Almansa, 14, 02006 Albacete, Spain. Tel./fax: þ34 967599316.
E-mail address: valentin.cena@gmail.com (V. Ceña).

Small interfering RNAs (siRNAs) are double-stranded RNA molecules that induce sequence-specific degradation of homologous single-stranded RNA [20]. The efficiency of siRNA and its limited side effects have made this technique an attractive alternative to the use of antisense oligonucleotides for therapies based on the inhibition of target genes [21]. Synthetic siRNAs are easy to deliver, require only small doses to produce their silencing effects, and can inactivate a gene at almost any stage in development [22]. It has been proposed that the efficiency of transfection for siRNA at the cellular level depends on cellular uptake, stability and endosomal escape. Various systems including polyethyleneimine, inorganic/metals, cationic lipids and dendrimers have been used for siRNA delivery to several cell types [23e25]. However, many of these systems do not achieve good transfection efficiency. Therefore, new, more efficient siRNA delivery systems that increase transfection efficiency are needed.

Previous results from our group have shown that CNHs can be used as a non-viral carrier to deliver siRNA [26]. In the present study, we synthesized and characterized a new CNH derivative using fourth-generation polyamidoamine (G4-PAMAM) dendrimers anchored to the CNH [27] surface and studied its efficiency to silence key proteins involved in the proliferation of prostate cancer cells and the effect of this silencing on the toxic actions of the antitumoral drug docetaxel.

2. Material and methods

2.1. Techniques

Microwave irradiations were carried out in a CEM DISCOVER S-Class reactor, with infrared pyrometer, pressure control system, stirring and an air-cooling option. The thermogravimetric analyses were performed with a TGA Q50 (TA Instruments) at 10 °C/min under N_2. For the TEM analyses a small amount of the functionalized CNHs was suspended in water and a drop of the suspension was placed on a copper grid (3.00 mm, 200 mesh, coated with carbon film). After air-drying, the sample was investigated by TEM, Philips EM 208, accelerating voltage of 100 kV.

2.2. Materials

Solvents were purchased from SDS and Fluka (Buchs, Switzerland). All dry solvents were freshly distilled under argon over an appropriate drying agent before use. Chemicals were purchased from SigmaeAldrich (Barcelona, Spain) or Acros Organics (Geel, Belgium) and used as received without further purification. Tert-butyl 6-(4-aminophenoxy)hexylcarbamate 1 was synthesized following the standard procedure found in the literature [28]. CNHs were produced by Carbonium s.r.l., Padova (Italy) by direct graphite evaporation in Ar flow, according to a patented method [29] and used without purification.

2.3. Synthesis of CNH derivatives

2.3.1. Boc-protected CNH intermediate

In a typical experiment, 20 mg of pristine CNHs (*p*-CNHs) were sonicated in deionized water together with 1 (2.05 g, 6.68 mmol) for 10 min in a microwave glass vessel. After that time, isoamyl nitrite (0.44 mL, 3.34 mmol) was added, and a condenser was put in place. The mixture was irradiated for 90 min at 80 °C at 100 W for 30 min, and after the addition of a new aliquot of isoamyl nitrite (0.44 mL, 3.34 mmol), at 30 W for 60 min at 80 °C. After cooling to room temperature, the crude was filtered on a Millipore membrane (PTFE, 0.2 mm). The collected black solid was washed using cycles of sonication and filtration with methanol and acetone until the filtrate was clear and ultimately dried under high vacuum, yielding 16.2 mg of Boc-protected CNH intermediate.

2.3.2. *f*-CNH1

HCl gas was bubbled for 5 min through a suspension of Boc-protected CNH intermediate (16.2 mg) in methanol (20 mL). The reaction mixture was stirred at room temperature for 14h, filtered on a Millipore membrane (GTTP, 0.2 mm) and washed by cycles of sonication and filtration using 50 mL of a mixture water/methanol (1:1). The collected black solid was dried under high vacuum, yielding 16 mg of *f*-CNH1.

2.3.3. *f*-CNH2

Twenty milligrams of *f*-CNH1 were sonicated in methanol for 5 min in a microwave glass vessel. Sonication was followed by the addition of *N*-ethyldiisopropylamine (1 mL, 4.83 mmol) and methyl acrylate (3 mL, 0.047 mmol), and the mixture was sonicated for 2 min. Finally, a condenser was put in place and the mixture was irradiated at 60 °C at 10 W for 60 min. After cooling to room temperature, the crude was filtered on a Millipore membrane (GTTP, 0.2 mm) and washed by cycles of sonication and filtration using 75 mL of a water/methanol mixture (1:1). The collected black solid was finally dried under high vacuum, yielding 20 mg of *f*-CNH2.

2.3.4. *f*-CNH3

10 mg of *f*-CNH2 were suspended in 10 mL of methanol and sonicated for 10 min, followed by the addition of the corresponding dendrimer: (0.015 mL of PAMAM dendrimer G4-NH_2 (10% w/v solution in methanol)). Next, a condenser was put in place and the reaction mixture was heated at 40 °C for 1 day. Subsequently, the crude was filtered on a Millipore membrane (GTTP, 0.2 mm) and washed by cycles of sonication and filtration using 75 mL of a water/methanol mixture (1:1). The collected black solid was dried under high vacuum, yielding 10 mg of *f*-CNH3.

2.4. Agarose gel retardation assay

Agarose gel electrophoresis was performed to analyze the siRNA (Qiagen, Valencia, CA) binding ability of *f*-CNH3 as previously described [30]. The *f*-CNH3/siRNA complexes were prepared at increasing N/P ratios (the molar ratio between the *f*-CNH3 amine groups and the siRNA phosphate groups) and incubated for 30 min at room temperature. For the N/P ratio calculation, we considered that only the outer primary amines of the G4-PAMAM dendrimers were protonated at the pH used in the experiments (5.5). Each sample was then loaded onto a 1.2% agarose gel containing ethidium bromide (0.05 mg/mL). Electrophoresis was performed at 60 mV for 15 min, and the resulting gels were photographed under UV-illumination. The binding capacity was evaluated based on the relative intensity of the free siRNA band in each gel lane with respect to the lane with naked siRNA.

2.5. siRNA release by polyanion competition

The ability of complexes to release siRNA after a challenge with the competing polyanionic heparin was determined as a measure of the ability of the dendriplex to be dissociated in an environment with an excess of negatively charged compounds, such as the cell interior [30]. Complexes were prepared as indicated above at a *f*-CNH3/siRNA N/P ratio of 7.5 to ensure complete binding of siRNA by the CNH derivative, and then incubated with increasing heparin sulfate concentrations (0, 1, 2, 4, 6, 8, and 10 mg/mg *f*-CNH3). The samples were run on an agarose gel as described above.

2.6. siRNA protection against RNAses

To study the protective actions of the dendriplex against siRNA cleavage by RNAses, *f*-CNH3/siRNA complexes, prepared at an N/P ratio of 7.5 as indicated above, or naked siRNA were incubated with 0.25% RNAase A for 30 min at 37 °C. Afterwards, RNAse was inactivated and the samples were incubated with an excess of heparin sulfate to ensure a complete siRNA release from the dendriplex as previously described [9]. Then, samples were loaded onto an agarose gel, under the same experimental conditions as the experiments described above.

2.7. *f*-CNH3/siRNA complex formation

Predesigned siRNA targeting human cofilin-1 (Hs_CFL1_3), and a control scrambled (SCR) siRNA targeting a sequence not sharing homology with the human genome (AllStars Negative Control) were purchased from Qiagen (Crawley, UK). LNCaP cells were transfected with siRNAs using the *f*-CNH3 as non-viral vector. Briefly, 15 mg/mL of *f*-CNH3 together with 100 nmol/L siRNA were incubated for 30 min at room temperature (15e25 °C) to form the transfection complexes. Cells, seeded on either 6- or 24-well plates, were 70e80% confluent at the time of transfection. RPMI-1640 medium was replaced with fresh medium and the *f*-CNH3/siRNA suspension was added to cells and incubated at 37 °C in a humidified atmosphere with 5% CO_2. For some experiments, after *f*-CNH3/siRNA transfection for 72 h, LNCaP cells were exposed to varying doses of docetaxel (1e50 nmol/L) for 24 h. Experiments were carried out three times unless otherwise specified.

2.8. Cell line and culture conditions

The human androgen-sensitive human PCa (LNCaP) cells were obtained from the American Type Culture and Collection (ATCC). LNCaP cells were routinely cultured in RPMI-1640 medium (Invitrogen, Carlsbad, CA) supplemented with 10% heat-inactivated fetal bovine serum (FBS; Invitrogen, Carlsbad, CA), 2 mmol/L L-glutamine (Invitrogen, Carlsbad, CA), 100 mg/ml streptomycin (Sigma, St. Louis, MO) and 100 IU/ml penicillin (Sigma, St. Louis, MO) in a 5% CO_2-humidified incubator at 37 °C.

2.9. siRNA uptake and toxicity

A fluorescein-labeled siRNA (siRNA-FAM, Qiagen, Crawley, UK) and propidium iodide (PI, Sigma, St. Louis, MO) were used to study the uptake of siRNA into LNCaP

cells and the toxicity of the complexes by flow cytometry. Briefly, complexes were prepared as described above. Cells were incubated with the *f*-CNH3/siRNA-FAM complexes or with naked siRNA-FAM at different time points (3e96 h). LNCaP cells were then washed twice with cold PBS (150 mM NaCl; 10 mM sodium phosphate, pH 7.4) and incubated with 5 mg/mL PI at 37 °C for 30 min in the dark. Next, cells were analyzed using a flow cytometer (BD-LSR, BD Biosciences, San Jose, CA). The percentage of positive cells was calculated by setting the background population as 98% negative when analyzing cells that had undergone transfection with siRNA-FAM alone. At least 10^4 cells were acquired for each condition. Data represent the mean SEM of 3 experiments.

2.10. Real-time RT-PCR analysis

RNA expression was evaluated by real-time RT-PCR in the LNCaP cell line as previously described [31]. Total RNA was extracted from cells using a commercially available reagent (Tripure, Sigma, St. Louis, MO) following the manufacturer's instructions. The concentration and quality of RNA was quantified by spectrophotometry (Infinite 200, Tecan, Salzburg, Austria) using one ml of the RNA sample. Total RNA was always checked by running an aliquot on an agarose gel to assess the integrity of the 18S and 28S mRNA bands. cDNA was synthesized from the purified total RNA using a High Capacity cDNA Reverse Transcription Kit (Applied Biosystems, Foster City, CA) according to the manufacturer's instructions. For real-time RT-PCR, cDNA was amplified using SYBR Green PCR Master mix with the StepOne Real-Time PCR System and the StepOne v2.0 software (Applied Biosystems, Foster City, CA). The primers used to amplify *cofilin-1* gene were 5′-TGTGGCTGTCTCTGATGGAG-3′ (forward) and 5′-TTGTCTGGCAGCATCTTGAC- 3′ (reverse). These sequences of primers had an annealing temperature of approximately 60 °C. The real-time RT-PCR reaction was maintained at 95 °C for 10 min, followed by 40 cycles of: 95 °C for 15 s and 60 °C for 1 min. The dissociation curves were analyzed to ensure the amplification of a single PCR product. In order to guarantee the reliability of the results, all samples were processed in triplicate. The quantification was performed by the comparative cycle threshold (Ct) method [32]. To normalize the data, the GAPDH RNA expression level was used as a housekeeping gene.

2.11. Lactate dehydrogenase (LDH) assay

LDH toxicity assays were performed by measuring the release of lactate dehydrogenase (LDH) into the culture medium using the CytoTox96® Non-Radioactive Cytotoxicity Assay kit (Promega, Madison, USA) as previously described [33]. Briefly, cells were treated with either *f*-CNH3/SCR siRNA or *f*-CNH3/cofilin-1 siRNA for 72 h. Afterwards, the medium was removed and cells were incubated with either vehicle or increasing doses of docetaxel (1e50 nmol/L) for 24 h. After the treatments, supernatants were collected and intact LNCaP cells were lysed using 0.1% (w/v) Triton X-100 in (0.9%) NaCl. Both LDH released to culture media, as well as LDH content within the cells were determined spectrophotometrically at 490 nm on a 96-well plate reader (Infinite 200, Tecan, Salzburg, Austria) following the manufacturer's instructions. LDH release (%) was defined by the ratio LDH released/total LDH present in the cells. Measurements were normalized between the mock treatment control and the Triton X-100 (0.1% w/v) control. All samples were run in quadruplicate.

2.12. Caspase-3 activity

Caspase-3 activity was determined as previously described [34]. Cells were treated with vehicle or complexes for 72 h. Afterwards, LNCaP cells were washed twice with cold PBS and lysed in a buffer containing 100 mmol/L *N*-2-hydroxyethyliperazine-*N*′-2-ethanesulphonic acid (HEPES), 5 mmol/L dithiothreitol (DTT), 5 mmol/L ethylene glycol-bis(b-aminoethyl ether)-*N,N,N*′,*N*′ ,-tetraacetic acid (EGTA), 0.04% Nonidet P-40 and 20% glycerol; pH 7.4. Extracts were centrifuged at 5000 × g for 10 min at 4 °C, and protein content was determined by the Bradford method (Pierce, Rockford, IL), using bovine serum albumin as a standard [35]. Cell extracts (30 mg of protein) were incubated in reaction buffer (25 mmol/L HEPES, 10% sucrose, 0.1% 3-[(3-cholamido propyl)-dimethylammonio]-2-hydroxy-1-propanesulfonic acid, 10 mmol/L DTT) containing 50 mmol/L fluorescence substrate Asp-Glu-Val-Asp-7-amino-4 trifluoromethyl-coumaryl (Z-DEVD-AFC) at 37 °C for 1 h. Cleavage of the AFC fluorophore was determined at 37 °C on an Infinite 200 microplate reader (Tecan, Salzburg, Austria) at an excitation wavelength of 400 nm and an emission wavelength of 505 nm.

2.13. Cell cycle analysis by flow cytometry

After the treatments, cells were trypsinized and collected by centrifugation. The cell pellets were washed with PBS and gently fixed with 75% ethanol before being placed in a freezer for 2 h. Cells were then collected by centrifugation, and the cell pellets were washed twice with PBS and resuspended in PBS containing 5 mg/mL PI and 50 mg/mL deoxyribonuclease-free ribonuclease A (Sigma, St. Louis, MO). The cell suspension was incubated in a dark room for 20 min at room temperature before cell cycle analysis with a BD-LSR flow cytometer (BD Biosciences, San Jose, CA). For each measurement, at least 10^4 cells were counted.

2.14. Cell proliferation assay

DNA synthesis in proliferating cells was determined by measuring 5-Bromo-2′-deoxy-uridine (BrdU) incorporation using the commercial 5-Bromo-2′-deoxy-uridine Labeling and Detection Kit III (Roche Molecular Biochemicals, Indianapolis, IN). To measure the cell proliferation rate, cells were seeded in 96-well plates and then incubated with either *f*-CNH3/SCR siRNA or *f*-CNH3/cofilin-1 siRNA during 72 h. Afterwards, the medium was removed and cells were incubated with either vehicle or increasing doses of docetaxel (1e50 nmol/L) for 24 h. After the treatments, LNCaP cells were pulse-labeled with 10 mmol/L BrdU for about 2 h at 37 °C and 5% CO_2. Quantitative determination of BrdU incorporated into cellular DNA was performed according to the manufacturer's instructions. Absorbance values were measured at 405 and 492 nm using an ELISA reader and each sample was run five times.

2.15. Statistical analysis

All data are expressed as mean SEM from at least 3 independent experiments. The nonparametric variance analysis (KruskaleWallis) followed by Dunn's test was used to evaluate statistical differences between groups. $p < 0.05$ was considered statistically significant. Statistical analyses were performed using SPSS 13.0 (SPSS, Chicago, IL).

3. Results

3.1. Synthesis and characterization of *f*-CNH3

Pristine CNHs (*p*-CNHs) are not soluble in water; therefore for biological applications functionalization of these nanostructures play a fundamental role, enhancing their solubility in aqueous media.

Scheme 1 describes the synthetic methodology to achieve the objective compound. First, we performed a radical addition of *tert*-butyl 6-(4-aminophenoxy)hexylcarbamate 1 in the presence of isoamyl nitrite as an oxidizing agent, using water as the solvent [28]. Boc deprotection in acidic media is necessary to release the amino groups and use them as focal points to allow the subsequent reaction with methyl acrylate in basic conditions. The double 1,4-addition provides the ester groups necessary for the linkage with the amino-terminated fourth-generation PAMAM dendrimer [26].

Fig. 1a shows the weight loss attributed to the attached organic materials onto the CNH surface. Each reaction step results in an increase in the molecular weight of these organic fragments, thus analysis of the weight loss reveals the number of functional groups added to the CNH surface in each reaction [36]. The first derivative (*f*-CNH1) shows a very high concentration of functional groups, corresponding to about one functional group every 73 carbon atoms of the CNH skeleton. In the case of the final derivative (*f*-CNH3), the functional group coverage decreases notably, to one functional group each 1755 carbon atoms of the CNH surface, but we must consider that the dendrimer is spatially very demanding, so it will cover several ester groups present on the surface.

f-CNHs were also investigated by transmission electron microscopy (TEM). A typical image is shown in Fig. 1b, indicating that the unique structures of CNHs as well as their spherical aggregates are preserved after the functionalization. Furthermore, images reveal that CNHs are well dispersed after functionalization.

As noted earlier, the introduction of functional groups enhances the solubility of CNHs. The dendrimer derivative *f*-CNH3 displays the highest dispersability (*f*-CNH3 0.1 mg/mL). This dispersability is due to the high number of positively charged ammonium groups located at the periphery of the PAMAM dendrimer.

3.2. Characterization of *f*-CNH3/siRNA complexes

Incubation of *f*-CNH3 with SCR siRNA showed complete binding of the siRNA at an N/P ratio of 7.5 as showed in Fig. 2A. In order to

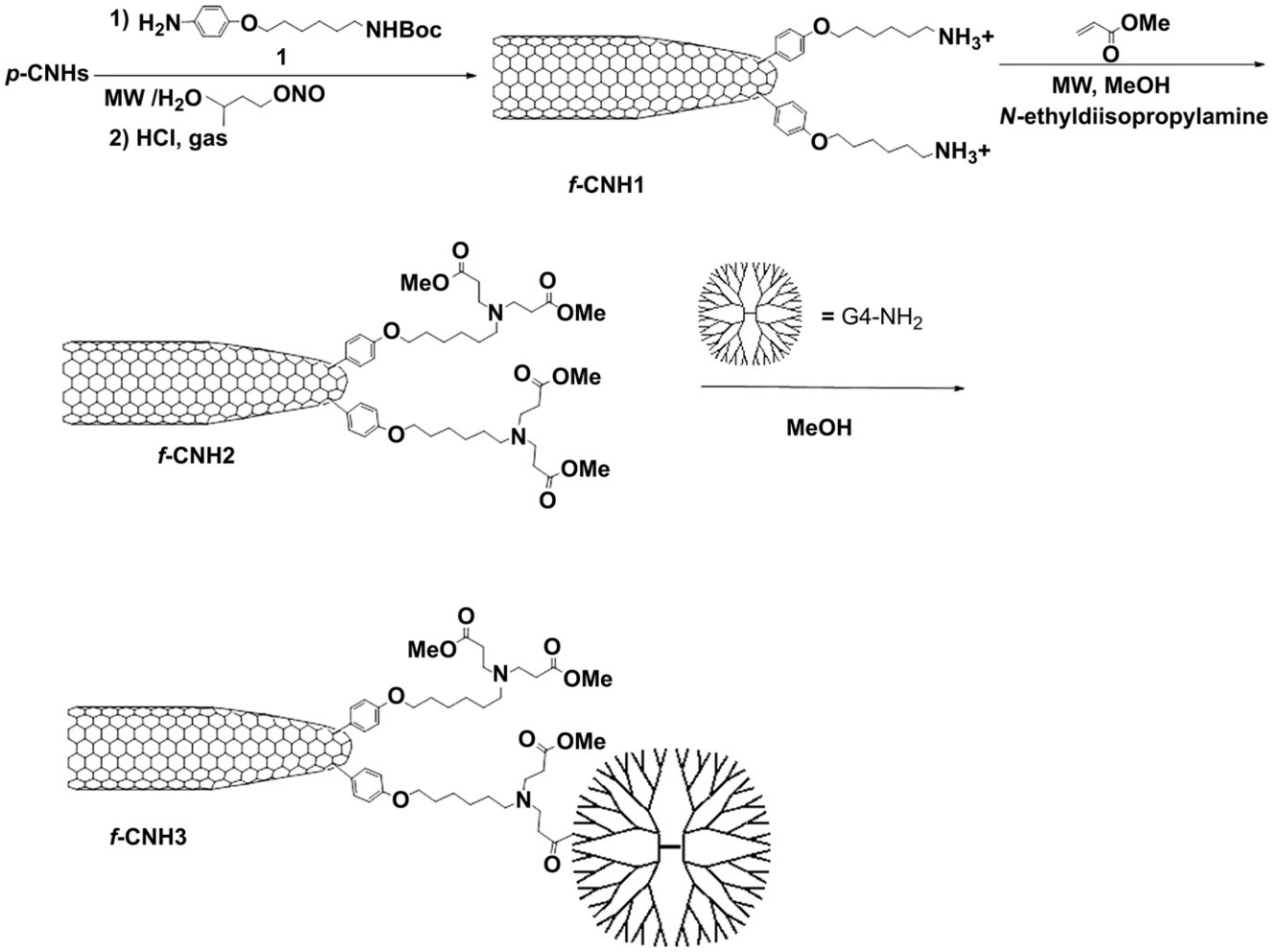

Scheme 1. Synthesis of the dendrimer-functionalized carbon nanohorns.

test the strength of the union between siRNA and dendrimer, heparin competition assays were performed (Fig. 2B). Complete siRNA release from complex was observed when the heparin (mg): *f*-CNH3 (mg) weight ratio reached 0.5 (Fig. 2B, lane 3). Moreover, siRNA bound to the hybrid material was protected from degradation by RNAase (Fig. 2C). These experiments indicate that *f*-CNH3 is able to bind siRNA and release it in the presence of the polyanion heparin (a treatment that resembles the intracellular environment) suggesting its ability to efficiently deliver siRNA to the cell interior.

3.3. *Transfection efficiency and toxicity of f-CNH3*

LNCaP cells were incubated with the complexes formed with 15 mg/mL *f*-CNH3 and 100 nmol/L siRNA-FAM for various times, and

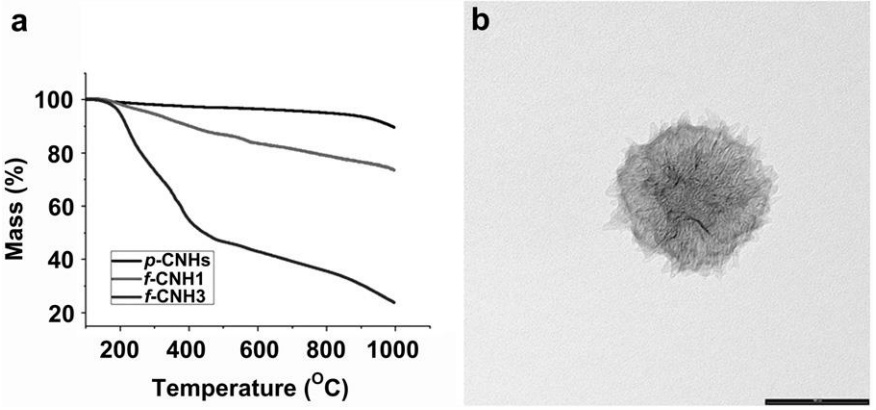

Fig. 1. a) Thermogravimetric analysis of pristine CNHs, *f*-CNH1 and *f*-CNH3 b) TEM images of *f*-CNH3, Scale bar corresponds to 100 nm.

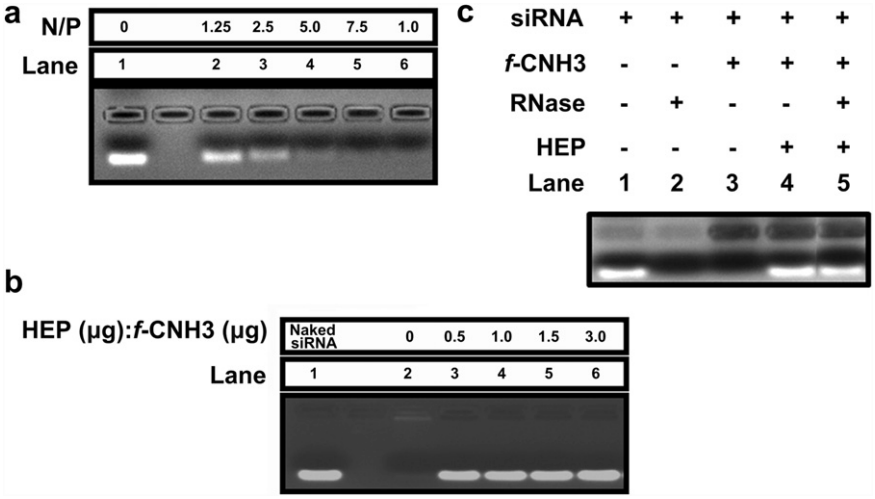

Fig. 2. *f*-CNH3/siRNA complex stability. A) Gel electrophoresis shift assay at the indicated N/P charge ratios. B) siRNA polyplexes stability against heparin (HEP) displacement. *f*-CNH3/siRNA complexes were formed at N/P ratio of 7.5 and incubated with varying concentrations of HEP (0, 0.5, 1, 1.5, and 3 mg/mg *f*-CNH3).C) *f*-CNH3/siRNA complexes formed at N/P ratio of 7.5 are able to prevent siRNA from 0.25% RNase A digestion.

transfection (FAM-labeled cells) and toxicity (PI positive cells) were analyzed by flow cytometry as indicated in Material and methods. LNCaP cells treated with siRNA-FAM alone showed very few FAM-positive cells (less than 2%) (Fig. 3). However, there was a time-dependent increase in the percentage of FAM-labeled cells reaching a 93.91 1.15% at 48 h and 97.51 1.16% at 72 h when the siRNA was delivered by the *f*-CNH3/siRNA complex (Fig. 3). The complexes lacked significant toxicity for up to 96 h (Fig. 3), indicating an increase in *f*-CNH3/siRNA complex internalization without toxicity by the LNCaP cells up to 96 h.

3.4. Cofilin-1 gene knockdown using *f*-CNH3/cofilin-1 siRNA complexes in LNCaP cells

Fig. 4 shows cofilin-1 mRNA levels quantified by real-time RT-PCR using total RNA extracted from LNCaP cells. *f*-CNH3/cofilin-1 siRNA complexes significantly decreased cofilin-1 mRNA levels to 22.04 2.01% and 31.75 12.5% at 72 h and 96 h post-treatment, respectively, when compared to untreated control LNCaP cells.

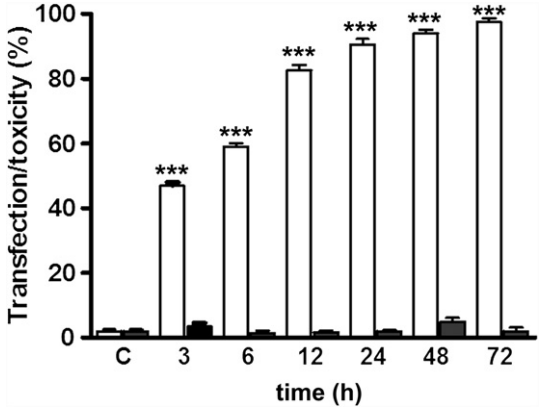

Fig. 3. Transfection efficiency (white bars) and toxicity (gray bars) of *f*-CNH3 as a non-viral delivery vector for siRNA in LNCaP cells. The cells were incubated with the complex formed by 15 mg/ml *f*-CNH3 and 100 nmol/L fluorescein-labeled siRNA (siRNA-FAM) for different times. Then, LNCaP cells were incubated with propidium iodide and analyzed by flow cytometry, as described in Material and methods. ***$p < 0.001$ as compared to Control cells (C).

The smaller effect observed at 96 h when compared to 72 h might reflects both the new cofilin mRNA synthesis and inactivation (or removal) of the delivered siRNA since only one application of the complex nanoparticle/siRNA was delivered to the prostate cancer cell culture. *f*-CNH3 alone, naked cofilin-1 siRNA or *f*-CNH3/SCR siRNA complex showed no decrease in cofilin-1 mRNA levels compared to control cells.

3.5. Knockdown of cofilin-1 enhanced apoptosis and cell death caused by docetaxel in LNCaP cells

Docetaxel treatment produced toxicity in LNCaP cells, as evidenced by a dose-dependent increment in caspase-3 activity (Fig. 5) and LDH released (Fig. 6) To examine the toxicity caused by silencing cofilin-1 along with docetaxel treatment, LNCaP cells were incubated for 72 h with or without *f*-CNH3/siRNA complexes and then exposed to docetaxel at concentrations ranging from 1 to 50 nmol/L for 24 h. Thus, docetaxel-induced LDH leakage into medium and caspase-3 activity was higher in cofilin-1 knockdown LNCaP cells than in either cells treated with *f*-CNH3/SCR siRNA complexes or untreated cells (Figs. 5 and 6).

3.6. Knockdown of cofilin-1 enhanced G_2/M arrest and decreased cell proliferation caused by docetaxel in LNCaP cells

Since docetaxel alone has been reported to cause severe mitotic arrest [37], we designed a sequential treatment regime that involved initial pretreatment with *f*-CNH3/siRNA complexes for 72 h to knockdown cofilin followed by the addition of increasing concentrations of docetaxel for 24 h to arrest the cell cycle and subsequently cellular proliferation.

Cell cycle analysis by flow cytometry showed that docetaxel treatment resulted in the accumulation of LNCaP cells in G_2/M phase in a dose-dependent manner indicating a decrease in tumoral cell proliferation (Fig. 7). Cofilin-1 gene knockdown using the *f*-CNH3/cofilin-1 siRNA complex significantly increased docetaxel-induced cell arrest in G2/M phase when compared with LNCaP cells treated with docetaxel alone, thus shifting the concentrationeresponse curve to the left (Fig. 7). The cofilin-1 siRNA effect in docetaxel-treated cells was sequence-specific because no effect was observed for the *f*-CNH3/SCR siRNA. This

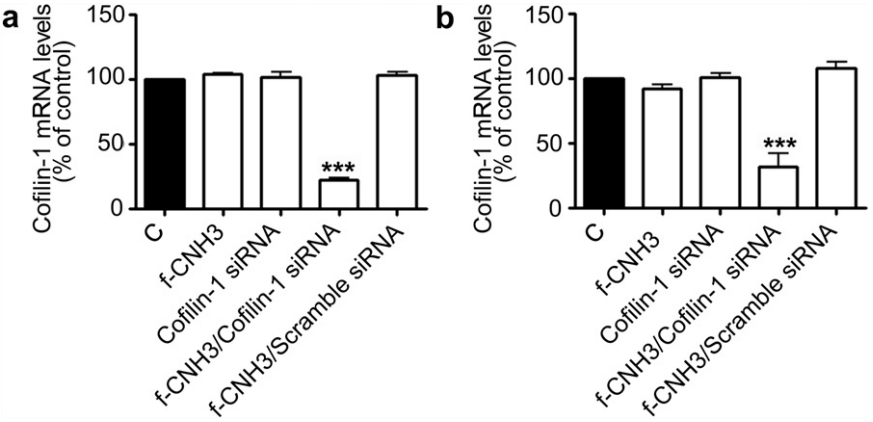

Fig. 4. Silencing effect of siRNA on cofilin-1 mRNA levels. The level of cofilin-1 mRNA was assessed by real-time RT-PCR. LNCaP cells were incubated with *f*-CNH3 alone, cofilin-1 siRNA alone and complex containing 15 mg/ml *f*-CNH3 and 100 nmol/L of either scramble siRNA or 100 nmol/L cofilin-1 siRNA for 72 h (A) and 96 h (B). Non-treated cells were used as control (C) and are represented as 100% of the signal. Data represent mean SEM of 3 independent experiments. ***$p < 0.001$ as compared to C.

indicates that cofilin-1 removal potentiates docetaxel antitumoral activity at low doses.

In addition, docetaxel (5e50 nmol/L) induced a significant inhibition of proliferation in LNCaP cells in a dose-dependent manner as measured by BrdU incorporation, which is consistent with the arrest in the G_2/M phase caused by the drug. These docetaxel-mediated inhibitory effects on cell proliferation were significantly enhanced using a *f*-CNH3/cofilin-1 siRNA complex (Fig. 8). These results were consistent with the results observed in the cell cycle analysis and, again, the potentiation of docetaxel-mediated cell cycle arrest was also sequence-specific because no effect was observed for the *f*-CNH3/SCR siRNA.

4. Discussion

Current treatment options for PCa are far from ideal. The tumor evolves from a hormone-sensitive to a hormone-independent stage and metastasizes; causing high mortality that makes this neoplasia one of the main causes of death among men in the Western world. Various attempts have been made to improve the chemotherapy by combining drugs that act on several targets required for the proliferation of the tumoral cells [19]. A different approach consists of combining an antitumoral drug with knocking down specific proteins required for proliferation and survival of the tumor cells using RNAi technology [9]. Here, we present data showing a potentiation of the antitumoral action of docetaxel on LnCaP human PCa cells using siRNA directed against the protein cofilin-1. The siRNA is delivered to the tumor cells by a new system consisting of G4-PAMAM dendrimers attached to a CNH. We found a potentiation of the antitumoral action of docetaxel by using a specific siRNA delivered to the cancer cell by the carbon-based system to knockdown the protein cofilin-1.

CNHs are a new type of material formed by graphene tubes that aggregate in structures of about 80e100 nm in diameter [27]. Their use in biological applications have several advantages over other carbon-based derivatives, such as their synthesis, which does not require catalysts, and their size, which allows their internalization

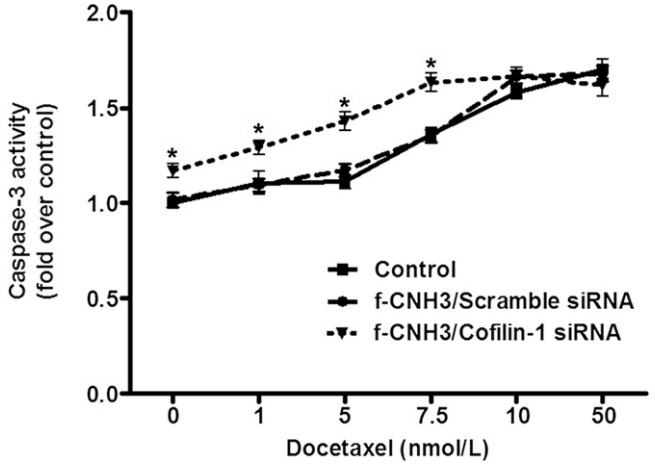

Fig. 5. Effect of cofilin-1 gene silencing on caspase-3 activity after docetaxel treatment. LNCaP cells were treated for 72 h with a complex containing 15 mg/ml of *f*-CNH3 and one of the following siRNAs: 100 nmol/L scramble siRNA or 100 nmol/L cofilin-1 siRNA. Then, cells were exposed to increasing doses of docetaxel (1e50 nmol/L) for 24 h. Caspase-3 activity was measured as described in Material and methods. Data represent mean SEM of 3 independent experiments. *$p < 0.05$ as compared to Control.

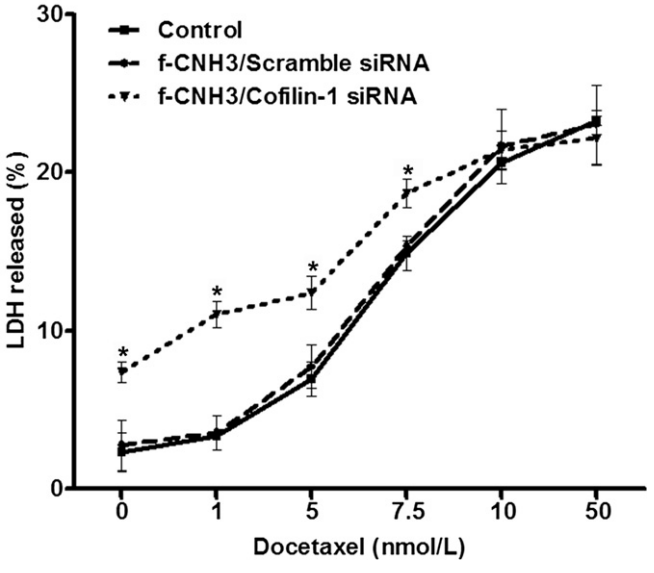

Fig. 6. Effect of cofilin-1 gene silencing on lactate deshydrogenase (LDH) released after docetaxel treatment. LNCaP cells were transfected for 72 h with 15 mg/ml *f*-CNH3/100 nmol/L scramble siRNA complex or 15 mg/ml *f*-CNH3/100 nmol/L cofilin-1 siRNA complex. Then, cells were incubated with increasing doses of docetaxel (1e50 nmol/L) for 24 h and the cellular viability was assayed by measuring the percentage of LDH released to the medium as described in Material and methods. Data represent mean SEM of 12 independent experiments. *$p < 0.05$ as compared to Control.

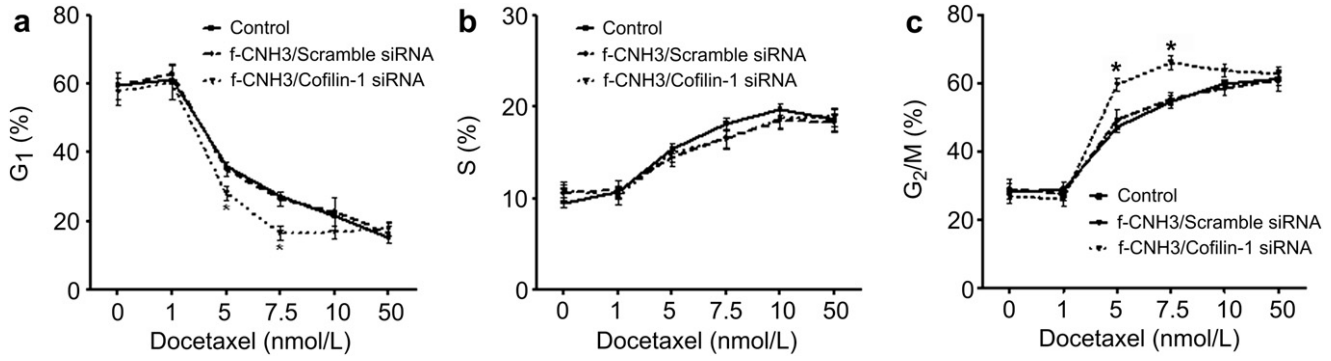

Fig. 7. Cell cycle analysis after docetaxel treatment of LNCaP cells silenced for cofilin-1. LNCaP cells were transfected for 72 h with 15 mg/ml *f*-CNH3/100 nmol/L scramble siRNA complex or 15 mg/ml *f*-CNH3/100 nmol/L cofilin-1 siRNA complex. Then, cells were incubated with increasing doses of docetaxel (1e50 nmol/L) for 24 h and analyzed by flow cytometry as described in Material and methods. Non-treated cells were used as Control (C). A) percentage of cells in G1 phase; B) percentage of cells in S phase; and C) percentage of cells in G2 þ M phases. Data represent mean SEM of 3 independent experiments. $^*p < 0.05$ as compared to C.

by endocytosis [38]. Functionalization of the CNH structures broadens their applications while enhancing their solubility in aqueous media [28,39] making them suitable as gene and drug delivery carriers. Here, we attached G4-PAMAM dendrimers to CNHs and explored the compound's ability to deliver specific siRNA to silence cofilin-1, a key protein involved in regulation of microtubules and involved in cell proliferation, in the androgen-dependent human PCa cell line LNCaP.

We observed that this new CNH derivative is able to bind siRNA and release it in the presence of an excess of the polyanion heparin, suggesting that the binding is reversible. Moreover, the binding to the CNH derivative protects the siRNA from degradation by RNAases. These 3 combined properties make this system suitable for genetic material delivery to cells in culture and likely in vivo [40]. The CNH derivative was able to enter more than 75% of the cells present in the culture and to deliver its siRNA cargo to the cells causing a decrease in both mRNA and protein levels for cofilin-1, indicating its efficiency as a siRNA delivery agent.

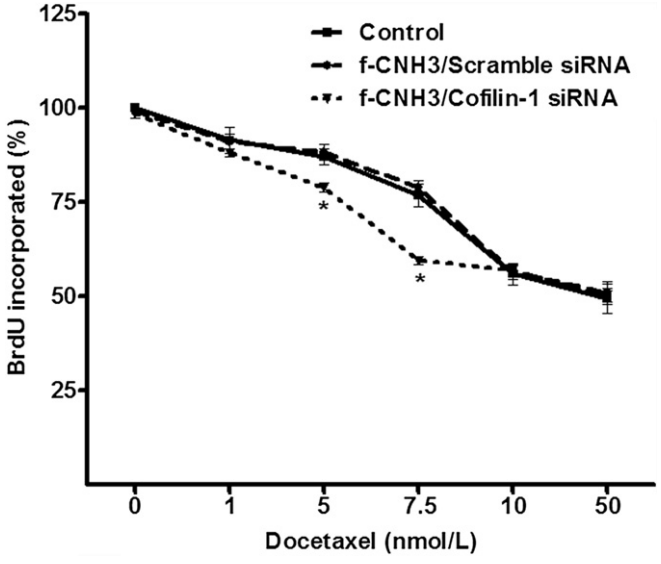

Fig. 8. Effect of cofilin-1 gene silencing on LNCaP cell proliferation after docetaxel treatment. LNCaP cells were transfected for 72 h with 15 mg/ml *f*-CNH3/100 nmol/L scramble siRNA complex or 15 mg/ml *f*-CNH3/100 nmol/L cofilin-1 siRNA complex. Then, cells were incubated with increasing doses of docetaxel (1e50 nmol/L) for 24 h. LNCaP cell proliferation was determined by 5-bromodeoxyuridine (BrdU) assay as described in Material and methods. Data represent mean SEM of 5 independent experiments. $^*p < 0.05$ as compared to Control.

Cofilin-1 has emerged as a key regulator of actin dynamics at the leading edge of motile cells [41]. It belongs to a family of F-actin depolymerizing factors with actin severing activity and that promotes actin dynamics by accelerating the treadmilling of actin filaments [42]. Thus, ADF/cofilin has been shown to regulate migration and chemotaxis in various cell types by cytoskeleton remodeling [43]. Accordingly, enhanced amounts of the actin-binding protein cofilin-1 have been associated with some types of tumors and metastases [12,44].

Here, we took advantage of the ability of the functionalized CNH derivative attached to G4-PAMAM dendrimers to deliver siRNA to human PCa cells to knockdown cofilin-1 and to explore whether this knockdown potentiates the effectiveness of the antitumoral drug docetaxel against these prostate cancer cells. Docetaxel is a member of the taxane drug family that is approved for the management of several cancers including PCa [45]. It promotes cell death by binding to b-tubulin and inhibiting its depolymerization, leading to modifications of the centrosome organization and acting on S, G2 and M phases of the cell cycle [46]. Knocking down expression of disease-related genes using siRNAs has the potential to treat a variety of illnesses including cancer [47,48]. Previous studies have reported that the suppression of cofilin expression with siRNA reduces the invasion of carcinoma cells by reducing the assembly and stability of invadopodia [44]. In addition, it has been shown that silencing the cofilin-1 gene in stromal cells markedly attenuated proliferation, adhesion and invasion of tumoral cells, but enhanced apoptosis [49].

Docetaxel concentrations show a sigmoidal relationship with the toxicity produced on PCa cells. The effects started at 1 nM and reached a plateau at 10 nM. Knocking down cofilin-1 potentiated the antitumoral actions of docetaxel shifting the concentrationeresponse curve to the left without increasing the maximum effect produced by docetaxel, probably because both treatments act on different targets of the same pathway. The development of therapies affecting multiple cell targets has been proposed as a strategy to overcome drug resistance in cancer therapy [50,51]. By reducing the required dose of each component, this association may increase efficiency while decreasing side effects. Moreover, combination therapy in cancer patients treated with a combination of different antitumoral drugs has been shown to have many advantages over single-agent therapies [50,51]. On the other hand, there is an emerging concept in PCa treatment in which it is likely that combining drugs acting on microtubules with drugs targeting different sites on the tubulin molecule may enhance treatment efficacy while reducing its toxicity [7,19].

5. Conclusion

This study demonstrates that a CNH derivative formed by a complex between a CNH and G4-PAMAM dendrimers is not toxic and can deliver a specific cofilin-1 siRNA to specifically inhibit the synthesis of this protein and modulate actin remodeling in tumoral cells *in vitro*, thus potentiating the antitumoral effects of docetaxel. Furthermore, these experiments support the hypothesis that siRNA treatment combined with classical anticancer drugs may represent a new approach for cancer therapy, providing the genetic material is coupled to the proper delivery system.

Acknowledgments

F.C.P-M. and B.C. are recipients of Torres Quevedo contracts from Ministerio de Ciencia e Innovación (Spain) and NanoDrugs, S.L. This work has been supported, in part, by grants BFU2011-30161-C02-01 from Ministerio de Ciencia e Innovación; PII1I09-0163-4002 and POII10-0274-3182 from Consejería de Educación, JCCM to V.C.

References

[1] Sakr WA, Grignon DJ, Crissman JD, Heilbrun LK, Cassin BJ, Pontes JJ, et al. High grade prostatic intraepithelial neoplasia (HGPIN) and prostatic adenocarcinoma between the ages of 20e69: an autopsy study of 249 cases. In Vivo 1994;8:439e43.

[2] Hankey BF, Feuer EJ, Clegg LX, Hayes RB, Legler JM, Prorok PC, et al. Cancer surveillance series: interpreting trends in prostate cancerepart I: evidence of the effects of screening in recent prostate cancer incidence, mortality, and survival rates. J Natl Cancer Inst 1999;91:1017e24.

[3] Sharifi N, Gulley JL, Dahut WL. Androgen deprivation therapy for prostate cancer. JAMA 2005;294:238e44.

[4] Petrylak DP. The current role of chemotherapy in metastatic hormone-refractory prostate cancer. Urology 2005;65:3e7.

[5] Chowdhury S, Burbridge S, Harper PG. Chemotherapy for the treatment of hormone-refractory prostate cancer. Int J Clin Pract 2007;61:2064e70.

[6] Fulton B, Spencer CM, Docetaxel. A review of its pharmacodynamic and pharmacokinetic properties and therapeutic efficacy in the management of metastatic breast cancer. Drugs 1996;51:1075e92.

[7] Li Y, Hong X, Hussain M, Sarkar SH, Li R, Sarkar FH. Gene expression profiling revealed novel molecular targets of docetaxel and estramustine combination treatment in prostate cancer cells. Mol Cancer Ther 2005;4:389e98.

[8] Mahon KL, Henshall SM, Sutherland RL, Horvath LG. Pathways of chemotherapy resistance in castration-resistant prostate cancer. Endocr Relat Cancer 2011.

[9] Monteagudo S, Perez-Martinez FC, Perez-Carrion MD, Guerra J, Merino S, Sanchez-Verdu MP, et al. Inhibition of p42 MAPK using a nonviral vector-delivered siRNA potentiates the anti-tumor effect of metformin in prostate cancer cells. Nanomedicine (Lond) 2012;7:493e506.

[10] Van Troys M, Huyck L, Leyman S, Dhaese S, Vandekerkhove J, Ampe C. Ins and outs of ADF/cofilin activity and regulation. Eur J Cell Biol 2008;87:649e67.

[11] Estornes Y, Gay F, Gevrey JC, Navoizat S, Nejjari M, Scoazec JY, et al. Differential involvement of destrin and cofilin-1 in the control of invasive properties of Isreco1 human colon cancer cells. Int J Cancer 2007;121:2162e71.

[12] Zhang Y, Tong X. Expression of the actin-binding proteins indicates that cofilin and fascin are related to breast tumour size. J Int Med Res 2010;38:1042e8.

[13] Ono S. Regulation of actin filament dynamics by actin depolymerizing factor/cofilin and actin-interacting protein 1: new blades for twisted filaments. Biochemistry 2003;42:13363e70.

[14] Abe H, Obinata T, Minamide LS, Bamburg JR. Xenopus laevis actin-depolymerizing factor/cofilin: a phosphorylation-regulated protein essential for development. J Cell Biol 1996;132:871e85.

[15] Zhu B, Fukada K, Zhu H, Kyprianou N. Prohibitin and cofilin are intracellular effectors of transforming growth factor beta signaling in human prostate cancer cells. Cancer Res 2006;66:8640e7.

[16] Posadas I, Perez-Martinez FC, Guerra J, Sanchez-Verdu P, Ceña V. Cofilin activation mediates Bax translocation to mitochondria during excitotoxic neuronal death. J Neurochem 2012;120:515e27.

[17] Debes JD, Tindall DJ. Mechanisms of androgen-refractory prostate cancer. N Engl J Med 2004;351:1488e90.

[18] Wang W, Eddy R, Condeelis J. The cofilin pathway in breast cancer invasion and metastasis. Nat Rev Cancer 2007;7:429e40.

[19] Pannu V, Karna P, Sajja HK, Shukla D, Aneja R. Synergistic antimicrotubule therapy for prostate cancer. Biochem Pharmacol 2011;81:478e87.

[20] Curtis CD, Nardulli AM. Using RNA interference to study protein function. Methods Mol Biol 2009;505:187e204.

[21] Golzio M, Mazzolini L, Ledoux A, Paganin A, Izard M, Hellaudais L, et al. In vivo gene silencing in solid tumors by targeted electrically mediated siRNA delivery. Gene Ther 2007;14:752e9.

[22] Perez-Martinez FC, Guerra J, Posadas I, Ceña V. Barriers to non-viral vector-mediated gene delivery in the nervous system. Pharm Res 2011;28:1843e58.

[23] Caminade AM, Turrin CO, Majoral JP. Dendrimers and DNA: combinations of two special topologies for nanomaterials and biology. Chemistry 2008;14: 7422e32.

[24] Mintzer MA, Simanek EE. Nonviral vectors for gene delivery. Chem Rev 2009; 109:259e302.

[25] Posadas I, Guerra FJ, Ceña V. Nonviral vectors for the delivery of small interfering RNAs to the CNS. Nanomedicine (Lond) 2010;5:1219e36.

[26] Guerra FJ, Herrero MA, Carrion B, Pérez-Martínez FC, Lucío M, Rubio N, et al. Carbon nanohorns functionalized with poltamidoamine dendrimers as efficient biocarrier materials for gene therapy. Carbon 2012;50:2832e44.

[27] Iijima S, Yudasaka M, Yamada R, Bandow S, Suenaga K, Kokai F, et al. Nano-aggregates of single-walled graphitic carbon nano-horns. Chem Phys Lett 1999:309.

[28] Rubio N, Herrero MA, Meneghetti M, Diaz-Ortiz A, Schiavon M, Prato M, et al. Efficient functionalization of carbon nanohorns via microwave irradiation. J Mater Chem 2009;19:4407e13.

[29] Schiavon M. Device and method for production of carbon nanotubes, fullerene and their derivatives. Patent US2004213727 (A1), 2004.

[30] Rodrigo AC, Rivilla I, Perez-Martinez FC, Monteagudo S, Ocaña V, Guerra J, et al. Efficient, non-toxic hybrid PPV-PAMAM dendrimer as a gene carrier for neuronal cells. Biomacromolecules 2011;12:1205e13.

[31] Perez-Carrion MD, Perez-Martinez FC, Merino S, Sanchez-Verdu P, Martinez-Hernandez J, Lujan R, et al. Dendrimer-mediated siRNA delivery knocks down Beclin 1 and potentiates NMDA-mediated toxicity in rat cortical neurons. J Neurochem 2012;120:259e68.

[32] Livak KJ, Schmittgen TD. Analysis of relative gene expression data using real-time quantitative PCR and the 2(-Delta Delta C(T)) Method. Methods 2001;25: 402e8.

[33] Posadas I, Lopez-Hernandez B, Clemente MI, Jimenez JL, Ortega P, de la Mata J, et al. Highly efficient transfection of rat cortical neurons using carbosilane dendrimers unveils a neuroprotective role for HIF-1alpha in early chemical hypoxia-mediated neurotoxicity. Pharm Res 2009;26:1181e91.

[34] Jordan J, Galindo MF, Tornero D, Benavides A, Gonzalez C, Agapito MT, et al. Superoxide anions mediate veratridine-induced cytochrome c release and caspase activity in bovine chromaffin cells. Br J Pharmacol 2002;137: 993e1000.

[35] Posadas I, Santos P, Blanco A, Munoz-Fernandez M, Ceña V. Acetaminophen induces apoptosis in rat cortical neurons. PLoS ONE 2010;5:e15360.

[36] Bom D, Andrews R, Jacques D, Anthony J, Chen BL, Meier MS, et al. Thermogravimetric analysis of the oxidation of multiwalled carbon nanotubes: evidence for the role of defect sites in carbon nanotube chemistry. Nano Lett 2002;2:615e9.

[37] Nehme A, Varadarajan P, Sellakumar G, Gerhold M, Niedner H, Zhang Q, et al. Modulation of docetaxel-induced apoptosis and cell cycle arrest by all- trans retinoic acid in prostate cancer cells. Br J Cancer 2001;84:1571e6.

[38] Fan XB, Tan J, Zhang GL, Zhang FB. Isolation of carbon nanohorn assemblies and their potential for intracellular delivery. Nanotechnology 2007;18: 195103.

[39] Pagona G, Karousis N, Tagmatarchis N. Aryl diazonium functionalization of carbon nanohorns. Carbon 2008;46:604e10.

[40] Yuan X, Shah BA, Kotadia NK, Li J, Gu H, Wu Z. The development and mechanism studies of cationic chitosan-modified biodegradable PLGA nanoparticles for efficient siRNA drug delivery. Pharm Res 2010;27:1285e95.

[41] Hotulainen P, Paunola E, Vartiainen MK, Lappalainen P. Actin-depolymerizing factor and cofilin-1 play overlapping roles in promoting rapid F-actin depolymerization in mammalian nonmuscle cells. Mol Biol Cell 2005;16:649e64.

[42] Chan AY, Bailly M, Zebda N, Segall JE, Condeelis JS. Role of cofilin in epidermal growth factor-stimulated actin polymerization and lamellipod protrusion. J Cell Biol 2000;148:531e42.

[43] Gungabissoon RA, Bamburg JR. Regulation of growth cone actin dynamics by ADF/cofilin. J Histochem Cytochem 2003;51:411e20.

[44] Yamaguchi H, Condeelis J. Regulation of the actin cytoskeleton in cancer cell migration and invasion. Biochim Biophys Acta 2007;1773:642e52.

[45] Petrylak DP, Tangen CM, Hussain MH, Lara Jr PN, Jones JA, Taplin ME, et al. Docetaxel and estramustine compared with mitoxantrone and prednisone for advanced refractory prostate cancer. N Engl J Med 2004;351:1513e20.

[46] Haldar S, Basu A, Croce CM. Bcl2 is the guardian of microtubule integrity. Cancer Res 1997;57:229e33.

[47] Ameyar-Zazoua M, Guasconi V, Ait-Si-Ali S. siRNA as a route to new cancer therapies. Expert Opin Biol Ther 2005;5:221e4.

[48] Leung RK, Whittaker PA. RNA interference: from gene silencing to gene-specific therapeutics. Pharmacol Ther 2005;107:222e39.

[49] Xu YL, Wang DB, Liu QF, Chen YH, Yang Z. Silencing of cofilin-1 gene attenuates biological behaviours of stromal cells derived from eutopic endometria of women with endometriosis. Hum Reprod 2010;25:2480e8.

[50] Woodcock J, Griffin JP, Behrman RE. Development of novel combination therapies. N Engl J Med 2011;364:985e7.

[51] Hu CM, Zhang L. Nanoparticle-based combination therapy toward overcoming drug resistance in cancer. Biochem Pharmacol 2012;83:1104e11.